Electron-impact excitation and ionization of atomic boron at low and intermediate energies

Kedong Wang*
College of Physics and Materials Science, Henan Normal University, Xinxiang 453007, People's Republic of China

Oleg Zatsarinny† and Klaus Bartschat‡
Department of Physics and Astronomy, Drake University, Des Moines, Iowa 50311, USA
(Received 5 February 2016; published 24 May 2016)

We present a comprehensive study of electron collisions with boron atoms by using the B-spline R-matrix method for electron energies ranging from threshold to 100 eV. Elastic, excitation, and ionization cross sections were obtained for all transitions between the lowest 11 states of boron. A multiconfiguration Hartree-Fock method with nonorthogonal term-dependent orbitals was employed to generate accurate wave functions for the target states. Close-coupling expansions including 13, 51, and 999 physical and pseudo-target states of boron were used to check the sensitivity of the results to changes in the theoretical model. The cross-section dataset obtained from the large-scale calculations is expected to be sufficiently accurate and comprehensive for most current modeling applications involving neutral boron.

DOI: 10.1103/PhysRevA.93.052715

I. INTRODUCTION

Accurate cross-section data for electron scattering from neutral boron atoms and boronlike ions are of significant practical importance, for example, for plasma diagnostics in astrophysics and thermonuclear fusion [1]. The boronization of plasma-exposed surfaces in tokamaks is an effective way to produce very pure fusion plasmas [2] by reduction of impurity influx [3]. To understand the erosion of materials with low atomic number Z, e.g., Be, B, and C, in the next generation of fusion experiments such as ITER [4], accurate and sufficiently complete datasets for electron collisions with these elements not only in their ground state, but also involving excited states, are needed for transport modeling.

For beryllium and carbon, extensive sets of calculations for excitation and ionization rates [5,6] or excitation cross sections [7] were carried out. For boron, on the other hand, much less has been done to date, and hence cross sections are only available within a narrow energy range and just for a few selected transitions. A likely reason for the lack of activity for this target is the major complication in the theoretical treatment of boron, which is caused by the presence of three active electrons above the $1s^2$ core. Consequently, atomic boron should be considered at least as a quasi-three-electron system, with substantial complications arising from significant coupling between the singly excited $2s^2 2p^2 n\ell$ states to states with a hole in the inner $2s$ subshell.

To our knowledge, the only currently available experimental data for electron-impact cross sections of neutral boron originate from the measurements by Kuchenev and Smirnov [8], who applied the method of intersecting electron and atomic beams. These data, however, were judged to be unreliable by Nakazaki and Berrington [9]. Based on relatively sophisticated (at the time) R-matrix (close-coupling) calculations for electron scattering from neutral boron, Nakazaki and Berrington suspected possible normalization problems regarding the absolute values reported in [8]. Marchalant *et al.* [10,11] later carried out an early R-matrix-with-pseudostates (RMPS [12]) calculation by including 60 physical and pseudostates in order to at least partially account for coupling to high-lying discrete Rydberg states as well as the ionization continuum. They reported results for elastic scattering and selected state-to-state excitation processes. Following this work, a much larger 640-state RMPS calculation was performed by Ballance *et al.* [13]. Electron-impact ionization cross sections for boron were generated by Kim and Stone [14] in the framework of the binary-encounter-Bethe (BEB) model. Finally, advanced nonperturbative time-dependent close-coupling (TDCC) and further RMPS calculations were carried out to determine the direct and total ionization cross sections of the outer two subshells ($2s$ and $2p$) of boron by Berengut *et al.* [15].

Most of the above results are available in the relatively narrow range of incident energies up to about 30 eV. Furthermore, the limited number of pseudostates included in the RMPS models, as well as the computational resources needed, did not allow for a thorough assessment of the quality of the calculated cross sections. The goal of the present work, therefore, was to provide an extensive dataset of cross sections for elastic scattering as well as electron-impact excitation and ionization of neutral boron, together with an estimate of their accuracy. The present calculations were performed with the B-spline R-matrix (BSR) method (for an overview, see [16]), employing an extended version of the associated computer code [17] that allows for the inclusion of a sufficient number of target pseudostates in the intermediate-energy regime. The distinctive feature of the method is the use of nonorthogonal one-electron orbital sets, both for the construction of the target wave functions and for the representation of the scattering functions. This allows us to generate accurate descriptions of the target structure and also helps avoiding the appearance of pseudoresonances at intermediate electron energies, which may have occurred in previous R-matrix calculations.

The present work is part of a series of extensive pseudostate calculations for electron scattering from atoms with a partially or fully occupied $2p$ outer shell, such as C [7], N [18], F

*wangkd@htu.cn
†oleg.zatsarinny@drake.edu
‡klaus.bartschat@drake.edu

[19], and Ne [20]. In many cases, we found a very strong influence of coupling to the target continuum on the predictions for transitions between low-lying discrete states. Along with the need to generate accurate target wave functions, properly accounting for this sensitivity is a crucial condition for obtaining accurate cross sections. For every model chosen, we always generate the entire set of meaningful cross sections, i.e., for elastic and inelastic transitions between all physical states as well as ionization from these states. Based on the comparison of predictions from different models with increasing number of target states, we then estimate the accuracy of the final results.

II. COMPUTATIONAL DETAILS

The target-structure calculations and the scattering calculations in the present work were carried out in a similar manner to our recent nonrelativistic R-matrix with pseudostates calculations [18] for atomic nitrogen. Consequently, we will only summarize the specific features for the present case below.

The target states of boron were generated by combining the multiconfiguration Hartree-Fock (MCHF) [21] and the B-spline box-based close-coupling (CC) methods [22]. The structure of the multichannel target expansion had the form

$$\begin{aligned}\Phi(2s^2nl,LS) &= \sum_{nl} a_{nl}^{LS,L'S'}\{\phi(2s^2,L'S')P(nl)\}^{LS} \\ &+ \sum_{nl,L'S'} b_{nl}^{LS,L'S'}\{\phi(2s2p,L'S')P(nl)\}^{LS} \\ &+ \sum_{nl,L'S'} c_{nl}^{LS,L'S'}\{\phi(2p^2,L'S')P(nl)\}^{LS} \\ &+ a\varphi(2s^22p)^{LS} + b\varphi(2s2p^2)^{LS} + c\varphi(2p^3)^{LS}. \qquad (1)\end{aligned}$$

Here $P(nl)$ denotes the orbital of the outer valence electron, while the ϕ and φ functions represent the configuration interaction (CI) expansions of the corresponding ionic and specific atomic states, respectively. Furthermore, L,S,L', and S' are the total orbital and spin angular momenta of the neutral and singly ionized system. It is advantageous to employ individual CI expansions for these states by directly including relaxation and term-dependence effects via state-specific one-electron orbitals. These expansions were generated in separate MCHF calculations for each state using the MCHF program [21]. They included all single and double excitations from the $2s$ and $2p$ orbitals to the $3l$ and $4l$ ($l = 0-3$) correlated orbitals. These multiconfiguration expansions ensure the proper inclusion of short-range correlations in the target wave functions. The resulting ionization potentials for all ionic states in Eq. (1) agree with the recommended values [23] to within 0.01 eV.

The unknown functions $P(nl)$ for the outer valence electron were expanded in a B-spline basis, and the corresponding equations were solved subject to the condition that the wave functions vanish at the boundary. The B-spline coefficients for the valence orbitals $P(nl)$, along with the various expansion coefficients in Eq. (1), were obtained by diagonalizing the N-electron atomic Hamiltonian. The number of spectroscopic bound states that can be generated in the above scheme depends on the B-spline (R-matrix) box radius. In most of the present calculations, the latter was set to $40\,a_0$, where $a_0 = 0.529 \times 10^{-10}$ m is the Bohr radius. We used 97 B splines of order 8 to span this radial range using a semiexponential knot grid. This allowed us to obtain good descriptions of the boron states with principal quantum number for the valence electron up to $n = 5$.

TABLE I. Binding energies (in eV) for the boron target states included in our CC expansion.

State	Term	NIST [23]	Present	Diff.
$2s^22p$	$^2P^o$	−8.298	−8.222	0.076
$2s2p^2$	^4P	−4.746	−4.698	0.048
$3s^23s$	^2S	−3.334	−3.306	0.028
$2s2p^2$	^2D	−2.365	−2.283	0.082
$2s^23p$	$^2P^o$	−2.271	−2.248	0.023
$2s^23d$	^2D	−1.508	−1.497	0.011
$2s^24s$	^2S	−1.478	−1.470	0.008
$2s^24p$	$^2P^o$	−1.134	−1.125	0.009
$2s^24d$	^2D	−0.860	−0.848	0.012
$2s^24f$	$^2F^o$	−0.856	−0.852	0.004
$2s^25s$	^2S	−0.841	−0.835	0.006

To keep the final expansions for the atomic states at a reasonable size, all target expansions were restricted by dropping contributions with coefficients the magnitude of which was less than the cutoff parameter of 0.01. Table I lists our calculated binding energies of the boron target states and compares them with the experimental data [23], which are based on the critical compilation by Kramida and Ryabtsev [24]. The overall agreement between our results and the NIST recommendations is satisfactory, with the deviations in the energy splittings being less than 0.1 eV for all states. It is possible to further improve the accuracy of the target binding energies by also taking into account excitations from the inner $1s$ shell. Such excitations, however, are not expected to be very important for low-energy scattering from the outer shells and hence were not included in the present calculations. In order to allow for a direct comparison between experiment and theory very close to the thresholds, we used the experimental values for the threshold energies in the scattering calculations.

The quality of our target description can be further assessed by comparing the results for the oscillator strengths of various transitions with experimental data and other theoretical predictions. Accurate oscillator strengths are very important to obtain reliable absolute values for the excitation cross sections, especially for optically allowed transitions at high incident electron energies. Table II shows the comparison of oscillator strengths between our calculated results and the recommended values from the NIST database [23]. For transitions involving principal quantum numbers $n = 2$ and 3, the NIST recommendations are based on the extensive MCHF calculations by Tachiev and Froese Fischer [25]. For higher-level transitions, the NIST-recommended values are based on the frozen-core R-matrix calculations of Fernley *et al.* [26].

The good agreement with other theoretical results (see, for example, Fuhr and Wiese [27] and the comprehensive citation

TABLE II. Oscillator strengths for selected dipole-allowed transitions in atomic boron.

Lower level	Upper level	f_L	f_L/f_V	NIST [23]
$(2s^2 2p)^2P^o$	$(2s^2 3s)^2S$	0.0803	1.01	0.0785
	$(2s^2 3d)^2D$	0.0172	0.99	0.0170
	$(2s^2 4s)^2S$	0.0162	0.98	0.0154
	$(2s^2 4d)^2D$	0.0762	1.01	0.0723
	$(2s^2 5s)^2S$	0.0117	0.96	0.0082
$(2s2p^2)^4P$	$(2p^3)^4S^o$	0.214	0.94	0.21
$(2s^2 3p)^2P^o$	$(2s^2 3s)^2S$	1.07	0.99	1.05
	$(2s^2 4s)^2S$	0.204	0.99	0.203
	$(2s^2 3d)^2D$	0.832	0.99	0.836

list of [23]) for these transitions suggests a high quality of the target description in the present calculations. The ratio of theoretical oscillator strengths obtained in the length (L) and velocity (V) forms of the electric dipole operator is also listed in Table II. This ratio is, to some extent, another quality indicator for the calculated f values. For all transitions listed, the length (f_L) and velocity (f_V) values agree within a few percent.

The expansion (1) is also able to generate continuum pseudostates that lie above the ionization threshold. The density and number of these states again depend on the box radius and, to a lesser extent, on other B-spline parameters, such as their order and distribution on the grid. The above approach is both a straightforward and general way to obtain the continuum pseudospectrum. It provides excellent flexibility by allowing us to vary the box radius or to change the density of the B-spline basis. The inclusion of the continuum pseudostates is extremely important to ensure the convergence of the final results for the excitation cross sections.

The scattering calculations were carried out by using a fully parallelized version of the BSR complex [17]. We set up several scattering models to check the convergence of the results. The first model, labeled BSR-13, includes 13 physical target states: the lowest 11 bound states of boron up to the $2s^2 5s$ state (as listed in Table I) plus the $2s$-excited states $(2s2p^2)^2S$ and $(2s2p^2)^2P$. The inclusion of the two latter states is important for the description of the strong $2s$-$2p$ transition. The next model, labeled BSR-51, additionally includes low-energy (up to 5 eV above the ionization threshold) $2s^2 kl$ continuum pseudostates for $2p$ ionization, as well as the $2p^3$ and $2s2p3l$ autoionizing states that result from excitations out of the $2s$ subshell. The main model, labeled BSR-999, finally extends the target continuum up to 50 eV above the ionization limit and includes all target states with orbital angular momenta $L \leqslant 4$. This scattering model also allows us to obtain the ionization cross sections. The maximum number of scattering channels was 2312. For a given B-spline basis, this number defines the size of the matrices involved, leading in the present case to generalized eigenvalue problems with matrix dimensions up to 200 000. This is essentially the limit that can be handled with our currently available computational resources.

We calculated partial waves for total orbital angular momenta up to $L_t = 25$ numerically and then used a top-up procedure to estimate the contribution to the transition-matrix elements from even higher L_t. Overall, with the various total spins and parities, this involved 156 partial waves. The calculation for the external region was performed with a parallelized version of the STGF program [28].

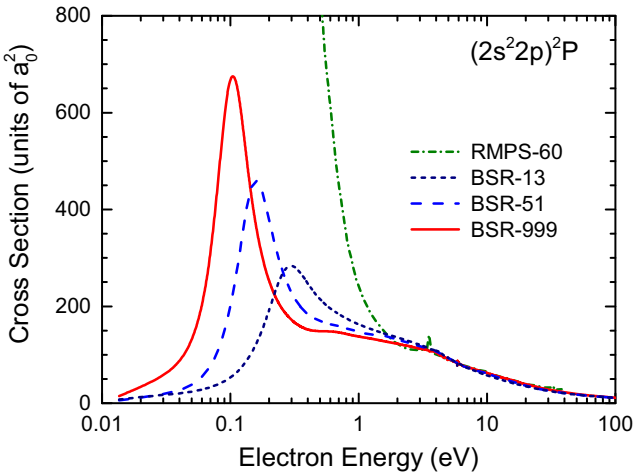

FIG. 1. Cross section for elastic electron scattering from boron atoms in their $(2s^2 2p)^2P$ ground state. The current BSR-13, BSR-51, and BSR-999 results are compared with earlier R-matrix-with-pseudostates (RMPS-60) calculations [11].

III. RESULTS AND DISCUSSION

A. Elastic cross sections

Results for the elastic cross section for electron scattering from the ground state of boron are presented in Fig. 1, where we compare the present results from the BSR-13, BSR-51, and BSR-999 models with those from an earlier RMPS calculation (RMPS-60) by Marchalant *et al.* [11]. All models yield very similar results for electron energies above 2 eV. For very low scattering energies, however, the predictions differ considerably. All present models suggest the existence of a strong near-threshold maximum related to the $(2s^2 2p^2)^1D$ state of B^-. The calculations predict a fast rise of the cross sections with increasing energy at low incident energies up to 0.1 eV, but the early RMPS-60 predictions are significantly higher than all present BSR results. Unfortunately, there are no experimental elastic cross-section data available for comparison.

Calculations for the low-lying $B^-(2s^2 2p^2)^1D$ shape resonance were carried out by many groups. The available results are listed in Table III. Johnson and Rohrlich [29] employed screened Z-dependent perturbation theory and a semiempirical extrapolation from ionization potentials. They suggested that the $B^-(2s^2 2p^2)^1D$ state is bound with respect to the ground state of neutral boron by 0.61 eV. Ten years later, Schaefer *et al.* [30] analyzed a number of negative ions, with particular emphasis on state-dependent correlation effects. Using empirical data, they concluded that a bound $B^-(2s^2 2p^2)^1D$ state does not exist. Instead, its position was estimated at 0.375 eV above the elastic threshold. Hunt and Moiseiwitsch [31] solved the Schrödinger equation with an empirically adjusted model potential. Employing scattering boundary conditions they obtained the position of the resonance as $E_r = 0.45$ eV and a width of $\tau = 0.11$ eV. Moser

TABLE III. Parameters of the identified B^- resonances (in eV).

Term	Energy	Width	Comments
$(2s^2 2p^2)^3P$	−0.280		Expt. [37]
	−0.289		BSR-999
$(2s^2 2p^2)^1D$	−0.61		[29]
	0.375		[30]
	0.45	0.11	[31]
	0.006		[32]
	0.275		[33]
	0.104 ± 0.008	0.068 ± 0.025	Expt. [34]
	0.095	0.054	[35]
	0.126	0.061	[36]
	0.104	0.082	BSR-999
$(2s^2 2p^2)^1S$	0.667	1.20	BSR-999
$2s2p^3)^5S^o$	2.480		[40]
	2.488	0	BSR-999
$(2s2p^3)^3D^o$	4.31	1.16	Expt. [38]
	4.012	1.223	BSR-999
$(2s2p^3)^3P^o$	4.968	0.007	BSR-999
$(2s2p^3)^1D^o$	6.802	0.155	BSR-999
$(2s2p^3)^1P^o$	8.462	0.040	BSR-999
$(2s2p^3)^3S^o$	9.017	0.234	BSR-999

and Nesbet employed the bound-state-type Bethe-Goldstone scheme of CI with all single and double excitations [32] and later also with configurational [33] excitations, respectively. The first calculation [32] predicted that the $B^-(2s^2 2p^2)^1D$ state is located essentially at the threshold (0.006 eV above), whereas the second calculation [33] found it at 0.275 eV above.

Experimental investigations for the parameters of this resonance were carried out by Lee *et al.* [34]. Based on their observations of resonance structures in electron detachment spectra arising from fast collisions of B^- ions with gas targets, they obtained the resonance position and width as 0.104 and 0.068 eV, respectively. In subsequent calculations, Sinanis *et al.* [35] computed the resonance parameters systematically in the framework of state-specific configuration interaction in the continuum and obtained a theoretical value consistent with the above measurement. Very recently, Tsednee and Yeager [36] applied the complex-scaled multiconfigurational spin-tensor electron propagator technique and obtained the B^- shape resonance parameters as $E_r = 0.126$ eV and $\tau = 0.061$ eV, again in reasonable agreement with the experimental result [34].

The present calculations clearly show that the theoretical position of this resonance is extremely sensitive to the number of channels included in the close-coupling expansion. The most extensive BSR-999 model predicts a strong ^1D resonance at 0.104 eV with a width of 0.082 eV. The position of the peak coincides with the measurement [34], and its width is within the uncertainty of the experimental value.

Our calculations also suggest the existence of a $B^-(2s^2 2p^2)^1S$ resonance the parameters of which are listed in Table III as well. This resonance, however, is very wide with a "peak" of much smaller magnitude. As a result, it is essentially covered by the high-energy wing of the strong ^1D resonance. For completeness, Table III also lists the parameters for the $B^-(2s^2 2p^2)^3P$ bound state of B^-. The close agreement with the experimental electron affinity [37] gives us further confidence in the quality of the present calculations.

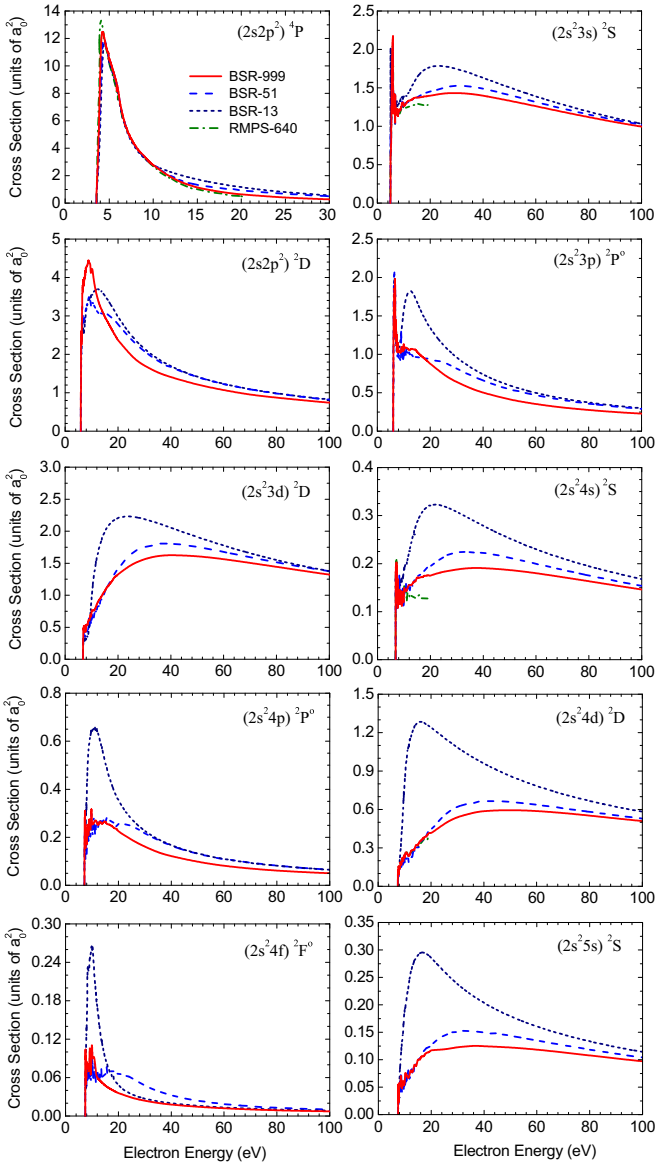

FIG. 2. Cross sections, as a function of collision energy, for electron-impact excitation of the first ten states of boron from the $(2s^2 2p)^2P$ ground state. The current BSR-13, BSR-51, and BSR-999 results are compared with the 640-state RMPS predictions of Ballance *et al.* [13].

B. Excitation cross sections

Excitation cross sections as a function of incident energy are presented in Fig. 2 for transitions from the ground state and in Fig. 3 for selected transitions between excited states. As mentioned above, three different close-coupling models (BSR-13, BSR-51, and BSR-999) were set up to check the convergence of the results. The cross sections are also compared with the most recent RMPS results of Ballance *et al.* [13]. However, since the latter data are only given for relatively low electron energies up to 20 eV, they do not allow us to

check the convergence at intermediate energies and thereby to analyze the potential influence of the target continuum.

For clarity of the presentation we do not compare the present cross sections with any other earlier results. Kuchenev and Smirnov [8] reported experimental excitation cross sections more than 20 years ago. It should be noted, however, that the experiment was not a direct measurement of the cross section, but rather a measurement of the radiation emitted from the decay of excited boron states, which were assumed to have been populated by direct electron excitation from the ground state. Cascade contributions from the excitation and decay of higher-lying states were not accounted for in the experiment. This may lead to unspecified uncertainties in the reported cross sections. As mentioned above, Nakazaki and Berrington [9] compared their R-matrix results with the measurements and suggested possible normalization problems with the absolute values given in [8]. Marchalant *et al.* [10,11] further improved the predictions of the total excitation cross sections, including up to 60 target states in the close-coupling expansion. Their cross sections were discussed in [13], and hence we will not compare them with the present results here.

The first transition from the ground state is a strong spin-forbidden exchange transition to the $(2s2p^2)^4P$ metastable state. In this case, excellent agreement is obtained between the results from all four models presented in Fig. 2. Convergence is hence evident over a wide range of incident-electron energies. We conclude that the theoretical cross section for this important transition has now been established to an accuracy of a few percent. In general, as seen from Fig. 3, only a small influence of channel-coupling effects was found for almost all exchange transitions from the $(2s2p^2)^4P$ levels. The cross sections for these cases exhibit a strong near-threshold maximum, with a steep decrease at higher energies. The target continuum has only a minor influence on the exchange transitions and also on other transitions that are dominated by short-range interactions. The notable exception is the very weak $(2s2p^2)^4P - (2s^23d)^2D$ transition, for which the maximum is shifted towards higher energies in the BSR-13 and BSR-51 models. This strong model sensitivity, which is typically for weak transitions, leads to significant differences in the predicted cross sections over a wide range of energies. Our BSR-999 results are in good agreement with the RMPS-640 calculations [13] in this case.

Compared to the exchange transitions, the convergence for the dipole transitions with respect to the number of states in the close-coupling expansion is much slower. This is clearly seen from the example of the transitions to the $n = 3$ states presented in Fig. 2. We conclude that the reduction of the calculated cross sections by 10–20% at intermediate energies in these cases is mostly due to coupling to the target continuum, since the coupling to the nearest discrete target states is already accounted for in the BSR-13 model.

For the transitions to the higher-lying $n = 4$ and 5 states, also presented in Fig. 2, both the BSR-999 and BSR-51 cross sections are considerably smaller than the BSR-13 results. In this case, the reductions are in the 20–75% range, with the largest effect seen for the $2p - 4d$ transition. This is caused by coupling to both the bound states and the target continuum.

The influence of the target continuum in electron collisions with atomic boron agrees well with the trend seen in our recent calculations for electron scattering from C [7], N [18], F [19], and Ne [20]. All these atoms have a partially or completely filled outer $2p$ subshell. Apparently, bound-continuum coupling effects are significant and increase with the occupation number of the subshell. Since all our scattering models employ the same target wave functions for the states included in the close-coupling expansion, we are able to directly draw conclusions about the importance of channel coupling in the collision model. Note that the accuracy of the target representation may also strongly influence the resulting excitation cross sections, as was illustrated for the case of electron scattering from C [7].

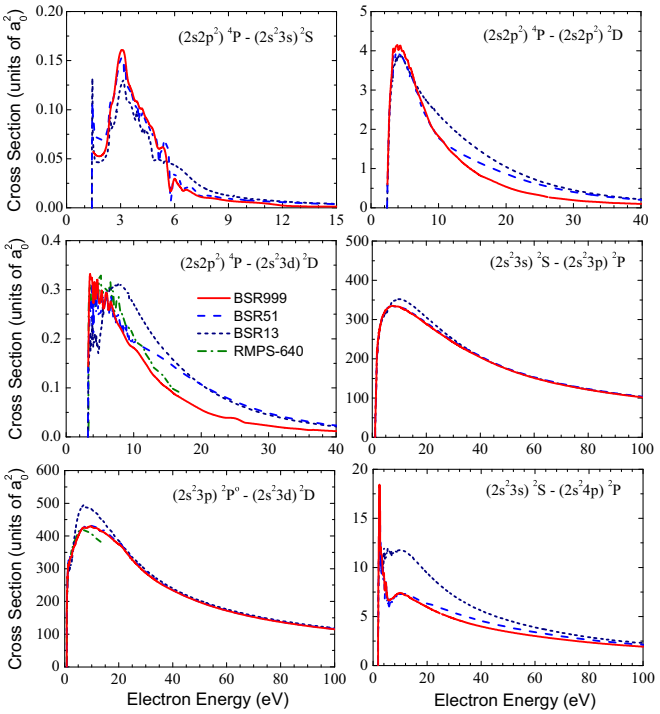

FIG. 3. Cross sections, as a function of collision energy, for selected electron-induced transitions from excited states of atomic boron. The current BSR-13, BSR-51, and BSR-999 results are compared with the 640-state RMPS predictions of Ballance *et al.* [13].

The cross sections for selected transitions between excited states are shown in Fig. 3. The general conclusions are similar to those for transitions from the ground state. Channel-coupling effects are often very small for strong transitions between close-lying levels, as illustrated, for example, by the $(2s^23s)^2S - (2s^23p)^2P^o$ and $(2s^23p)^2P^o - (2s^23d)^2D$ transitions. However, the $(2s^23s)^2S - (2s^24p)^2P^o$ transition shows that coupling to nearby levels can be strong enough to reduce the predicted cross sections by up to 30%. In general, coupling to the continuum for transitions between excited states is less important than for transitions from the ground state.

For low incident-electron energies, we obtain reasonable agreement with the RMPS results of Ballance *et al.* [13]. The small remaining differences between the two sets of predictions can likely be attributed to the different representations of the target structure. Given the well-known trends associated with the inclusion of additional pseudostates, we believe that

the present BSR-999 model yields the most reliable cross sections.

While resonance contributions to the excitation cross sections are relatively small overall, a few prominent structures can be seen in the near-threshold regime. Specifically, the partial-wave analysis reveals that the dominant threshold peak for the $(2s^2 2p)^2P^o - (2s2p^2)^4P$ transition is due to the strong $(2s2p^3)^3D^o$ shape resonance. Distinctive resonance features can also be seen in the excitation of the $3s$ and $3p$ levels. The most significant resonances are associated with the strong $2s$-$2p$ transition and have the dominant configuration $2s2p^3$. Their parameters, as derived from an eigenphase analysis, are given in Table III. Some of these resonances with terms $^3D^o$, $^3P^o$, and $^3S^o$ also have a strong influence on the photodetachment process [39].

Finally, it is worth mentioning that we obtained close agreement with the MCHF calculations [40] for the position of the metastable $B^-(2s2p^3)^5S^o$ state, which is located well below the $(2s2p^2)^4P$ states. In light of the selection rules for conservation of the total spin in nonrelativistic models, this state has no influence on electron scattering. However, it was detected as the lowest R-matrix pole of the $^5S^o$ symmetry.

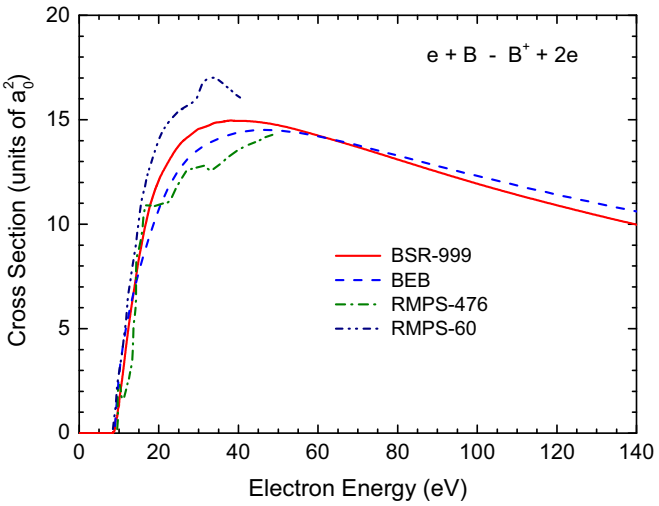

FIG. 4. Electron-impact total ionization cross section for the $(2s^2 2p)$ ground state of boron. The current BSR-999 results are compared with 476-state RMPS [15], 60-state RMPS [11], and BEB predictions [14].

C. Ionization cross sections

Cross sections for electron-impact ionization of the boron ground state are presented in Fig. 4. The BSR-999 total ionization cross sections were obtained as the sum of the excitation cross sections to all target states above the first ionic ground state. This includes the direct contribution from the continuum pseudostates plus an appropriate portion from excitation of quasidiscrete states in the continuum, i.e., from excitation-autoionization. For boron, the contribution from the latter process originates mainly from the set of $2s \rightarrow nl$ ($n \geqslant 2$) one-electron transitions. We assumed that the radiative decay of the autoionizing states is negligible in comparison to the autoionization channel.

We are not aware of any experimental data for the ionization of neutral boron. Figure 4, therefore, compares our ionization cross sections with a few other theoretical predictions. The present BSR results are in good agreement with the semiempirical BEB predictions of Kim and Stone [14] over a wide range of energies from threshold to 150 eV. At low energies, our results are found to lie slightly above the RMPS-476 predictions of Berengut *et al.* [15], but below the previous RMPS-60 results of Marchalant *et al.* [10]. The not-entirely-smooth energy dependence of the RMPS results is likely due to the low-density distribution of the continuum pseudostates and/or the occurrence of pseudoresonances. We believe that the large number of pseudostates in the present BSR-999 model and the practically complete elimination of pseudoresonance structure provides a very accurate representation of continuum-coupling effects.

More details regarding the ionization process are represented in Fig. 5, in which we exhibit the direct ionization cross sections for the $2s$ and $2p$ subshells together (except near threshold, individually $2s$ ionization contributes about 25% for most energies), along with the contribution from the $(2s2p^2)^2P$ autoionizing state. The latter clearly reveals the importance of the excitation-autoionization process due to the strong $2s$-$2p$ transition. As seen from the figure, the process contributes approximately 40% compared to direct ionization. Starting at around 35-eV incident energy, our direct cross sections are systematically lower than the BEB predictions. It is conceivable that the accuracy of our results deteriorates in this regime, also due to the limited energy range (up to 50 eV) covered by the pseudostates. The TDCC results generally lie above our predictions, by up to 20% at intermediate energies. This difference can likely be attributed to the treatment of initial-state correlation effects. We employ an extensive multiconfiguration expansion, whereas a single-configuration representation was used in the TDCC calculations. A similar

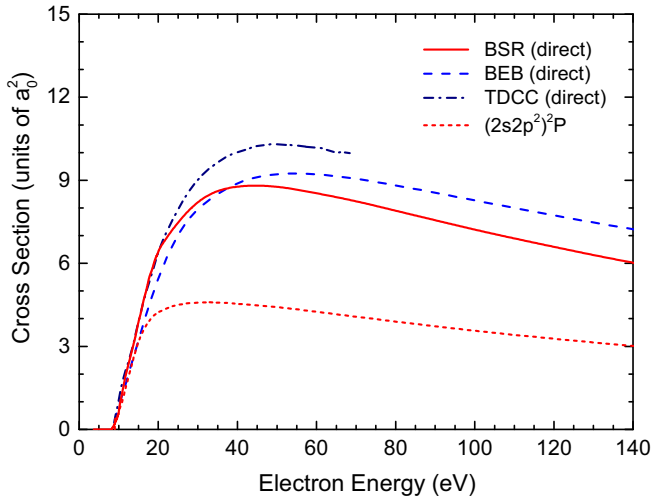

FIG. 5. Electron-impact direct ionization cross sections of the $(2s^2 2p)$ ground configuration of boron. The present BSR-999 results are compared with the BEB predictions of Kim and Stone [14] and the TDCC results of Berengut *et al.* [15]. Also shown is the contribution from the $(2s2p^2)^2P$ autoionizing state.

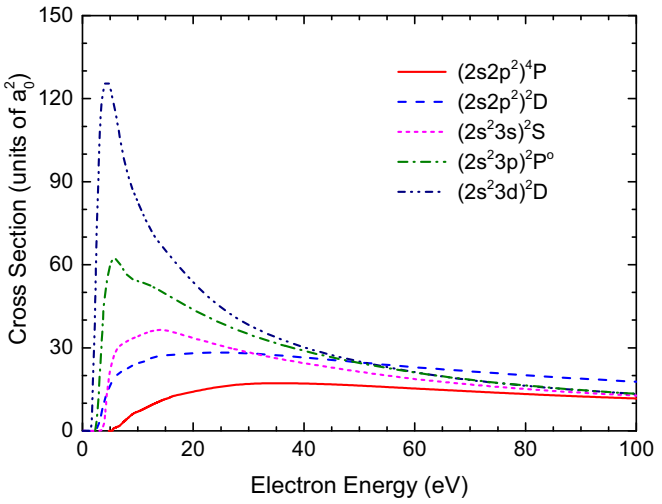

FIG. 6. Electron-impact ionization cross sections for the first five excited states of boron, as obtained in the BSR-999 model.

difference between BSR and TDCC results was observed for neon [41].

The ionization cross sections from the first five excited states of boron are presented in Fig. 6. Along with the ionization of the ground state, the cross section for ionization from the metastable $(2s2p^2)^4P$ state is of particular importance for plasma modeling. The latter is close in magnitude to that of the ground state, while ionization of the $(2s2p^2)^2D$ state is even more likely due to its lower ionization potential. Some of the $2s^2nl$ cross sections exhibit a near-threshold maximum, which is characteristic for ionization of excited states. In all these cases, ionization occurs mainly via removal of the outermost valence electron.

D. Grand-total cross section

We conclude the presentation of our results with Fig. 7, which exhibits the grand total cross section for electron collisions with boron atoms in their $(2s^22p)^2P^o$ ground state. This is the sum of the angle-integrated elastic, excitation, and ionization cross sections. The elastic cross section provides the largest contribution at low energies, while the contributions from ionization become almost equivalent to those from elastic scattering at energies above 50 eV. Overall, excitation processes never contribute more than 15% to the grand total cross section.

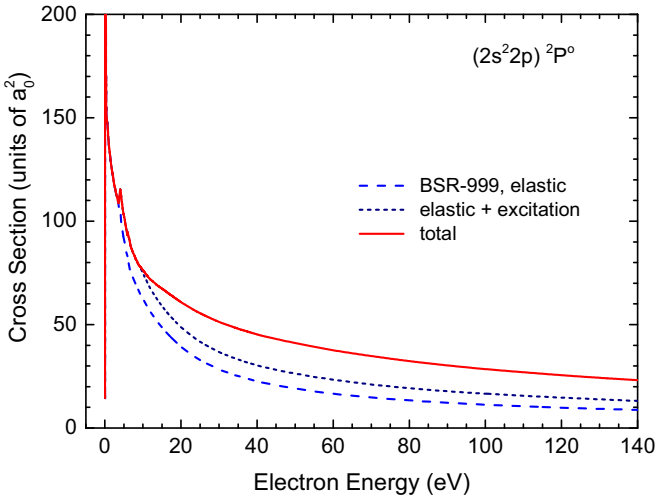

FIG. 7. Elastic, elastic + excitation, and grand total cross section for electron collisions with atomic boron in the B$(2s^22p)$ ground state, as obtained in the BSR-999 model.

IV. SUMMARY AND CONCLUSIONS

We have carried out a detailed study of electron collisions with neutral boron, including elastic scattering, excitation, and ionization processes from the ground and several excited states. State-to-state excitation cross sections were obtained for all transitions between the lowest 11 states of boron. While only a small number of selected results could be presented in this paper, the entire dataset is available in electronic form upon request.

The calculations were performed with the BSR code [17]. The particular advantage of the approach is the possibility to optimize the various atomic wave functions individually by employing term-dependent nonorthogonal one-electron orbitals in the description of the target states.

Emphasis in the present calculations was placed on estimating the likely accuracy of the final results. In order to check such important effects as target polarization and the influence of coupling to the target continuum, we compared the results from our most extensive calculations, which included 999 target states, with those from two smaller models that included just 13 physical bound states or 51 bound plus pseudotarget states. The differences between the results from these models provided an indication regarding the convergence of the close-coupling expansion for the problem at hand. While certainly not negligible at intermediate energies, overall the influence of the target continuum was found to be significantly less than seen before for atoms with a partially filled $2p$ shell, particularly C [7], N [18], and F [19]. While this may not be too surprising for discrete transitions that conserve the total spin, the stability of spin-forbidden transitions involving the $(2s2p^2)^4P$ state and a series of singly excited doublet states with configuration $(2s^2n\ell)$ is noteworthy. Furthermore, we predicted the elastic cross section at very low incident energies, where a prominent near-threshold resonance was detected.

Our best model, BSR-999, was also used to calculate the electron-impact direct ionization cross section for the boron ground state. Good agreement for this cross section was obtained with that predicted by the semiempirical BEB approach. On the other hand, our direct ionization cross sections are significantly different from the corresponding TDCC results, presumably because of inner-state correlations that the target description used in the TDCC approach cannot account for to sufficient extent. The excitation-autoionization contribution for ground-state ionization was found to be very important. Finally, the grand total cross section from the ground state, together with the contributions from elastic scattering, excitation, and ionization, was presented.

We expect the cross sections presented here to be useful for many practical applications. Comparison of our results with those from earlier RMPS calculations, which were carried out independently from the present work (albeit only in the low-energy regime), leads us to conclude that the excitation cross sections for the most important (for modeling purposes) transitions from the ground state $(2s^2 2p)^2P$ and the metastable $(2s2p^2)^4P$ state have now been established to an accuracy of a few percent over the energy range considered in this work.

ACKNOWLEDGMENTS

This work was supported by the NSF under Grants No. PHY-1212450, No. PHY-1403245, and No. PHY-1520970, and by the XSEDE supercomputer Allocation No. PHY-090031. The large calculations were carried out on Stampede at the Texas Advanced Computing Center. K.W. was sponsored by the China Scholarship Council and would like to thank Drake University for the hospitality during his visit.

[1] Y. Itikawa, K. Takayanagi, and T. Iwai, At. Data Nucl. Data Tables **31**, 215 (1984).
[2] J. Winter, L. Grobusch, T. Rose, J. V. Seggern, H. G. Esser, and P. Wienhold, Plasma Sources Sci. Technol. **1**, 82 (1992).
[3] B. Wan, Y. Zhao, J. Li, M. Song, Z. Wu, J. Luo. C. Li, and X. Wang, Plasma Sources Sci. Technol. **4**, 1375 (2002).
[4] `https://www.iter.org`.
[5] J. Colgan, S. D. Loch, M. S. Pindzola, C. P. Ballance, and D. C. Griffin, Phys. Rev. A **68**, 032712 (2003).
[6] C. P. Ballance, D. C. Griffin, J. Colgan, S. D. Loch, and M. S. Pindzola, Phys. Rev. A **68**, 062705 (2003).
[7] Y. Wang, O. Zatsarinny, and K. Bartschat, Phys. Rev. A **87**, 012704 (2013).
[8] A. K. Kuchenev and Y. M. Smirnov, Opt. Spectrosc. **51**, 116 (1981).
[9] S. Nakazaki and K. A. Berrington, J. Phys. B **24**, 4263 (1991).
[10] P. Marchalant, K. Bartschat, K. Berrington, and S. Nakazaki, J. Phys. B **30**, L279 (1997).
[11] P. Marchalant and K. Bartschat, J. Phys. B **30**, 4373 (1997).
[12] K. Bartschat, E. T. Hudson, M. P. Scott, P. G. Burke, and V. M. Burke, J. Phys. B **29**, 115 (1996).
[13] C. P. Ballance, D. C. Griffin, K. A. Berrington, and N. R. Badnell, J. Phys. B **40**, 1131 (2007).
[14] Y. K. Kim and P. M. Stone, Phys. Rev. A **64**, 052707 (2001).
[15] J. C. Berengut, S. D. Loch, M. S. Pindzola, C. P. Ballance, and D. C. Griffin, Phys. Rev. A **76**, 042704 (2007).
[16] O. Zatsarinny and K. Bartschat, J. Phys. B **46**, 112001 (2013).
[17] O. Zatsarinny, Comput. Phys. Commun. **174**, 273 (2006).
[18] Y. Wang, O. Zatsarinny, and K. Bartschat, Phys. Rev. A **89**, 062714 (2014).
[19] V. Gedeon, S. Gedeon, V. Lazur, E. Nagy, O. Zatsarinny, and K. Bartschat, Phys. Rev. A **89**, 052713 (2014).
[20] O. Zatsarinny and K. Bartschat, Phys. Rev. A **86**, 022717 (2012).
[21] C. Froese Fischer, Comput. Phys. Commun. **176**, 559 (2007).
[22] O. Zatsarinny and C. Froese Fischer, Comput. Phys. Commun. **180**, 2041 (2009).
[23] A. Kramida, Yu. Ralchenko, J. Reader, and NIST ASD Team (2015), NIST Atomic Spectra Database, ver. 5.3, http://physics.nist.gov/asd (28 April 2016), National Institute of Standards and Technology, Gaithersburg, MD.
[24] A. E. Kramida and A. N. Ryabtsev, Phys. Scr. **76**, 544 (2007).
[25] G. Tachiev and C. Froese Fischer, J. Phys. B **33**, 2419 (2000).
[26] J. A. Fernley, A. Hibbert, A. E. Kingston, and M. J. Seaton, J. Phys. B **32**, 5507 (1999).
[27] J. R. Fuhr and W. L. Wiese, J. Phys. Chem. Ref. Data **39**, 013101 (2010)
[28] N. R. Badnell, J. Phys. B **32**, 5583 (1999); see also http://amdpp.phys.strath.ac.uk/UK_RmaX/codes.html.
[29] H. R. Johnson and F. Rohrlich, J. Chem. Phys. **30**, 1608 (1959).
[30] H. F. Schaefer III, R. A. Klemm, and F. E. Harris, J. Chem. Phys. **51**, 4643 (1969).
[31] J. Hunt and B. L. Moiseiwitsch, J. Phys. B **3**, 892 (1970).
[32] C. M. Moser and R. K. Nesbet, Phys. Rev. A **4**, 1336 (1971).
[33] C. M. Moser and R. K. Nesbet, Phys. Rev. A **6**, 1710 (1972).
[34] D. H. Lee, W. D. Brandon, D. Hanstorp, and D. J. Pegg, Phys. Rev. A **53**, R633 (1996).
[35] C. Sinanis, Y. Komninos, and C. A. Nicolaides, Phys. Rev. A **57**, R3158 (1998).
[36] T. Tsednee and D. L. Yeager, Phys. Rev. A **91**, 063405 (2015).
[37] T. Andersen, H. K. Haugen, and H. Hotop, J. Phys. Chem. Ref. Data **28**, 1511 (1999).
[38] P. Kristensen, H. H. Andersen, P. Balling, L. D. Steele, and T. Andersen, Phys. Rev. A **52**, 2847 (1995).
[39] K. Wang, O. Zatsarinny, and K. Bartschat, Eur. Phys. J. D **70**, 72 (2016).
[40] C. Froese Fischer, J. Phys. B **29**, 1169 (1996).
[41] O. Zatsarinny and K. Bartschat, Phys. Rev. A **85**, 062710 (2012).